WILEY ECOLOGY

Bayesian hierarchical modeling of size spectra

Journal:	*Ecology*
Manuscript ID	Draft
Wiley - Manuscript type:	Statistical Report
Date Submitted by the Author:	n/a
Complete List of Authors:	Wesner, Jeff; University of South Dakota, Pomeranz, Justin; University of Canterbury, Biology Junker, James; Michigan Technological University, Great Lakes Research Center Gjoni, Vojsava; University of South Dakota, Biology Lio, Yuhlong; University of South Dakota, Mathematics
Substantive Area:	Statistics (general) < Statistics and Modeling < Theory < Substantive Area, Community Analysis/Structure/Stability < Community Ecology < Substantive Area
Organism:	
Habitat:	
Geographic Area:	
Key words/phrases:	Bayesian, body size spectra, hierarchical, Pareto, power law, Stan
Abstract:	A fundamental pattern in ecology is that smaller organisms are more abundant than larger organisms. This pattern is known as the individual size distribution (ISD), which is the frequency of all individual sizes in an ecosystem, regardless of taxon. The ISD is described by power law distribution with the form $f(x) = Cx^{\lambda}$, and a major goal of size spectra analyses is to estimate the ISD parameter λ. However, while numerous methods have been developed to do this, they have focused almost exclusively on estimating λ from single samples. Here, we develop an extension of the truncated Pareto distribution within the probabilistic modeling language Stan. We use it to estimate multiple ISD parameters simultaneously with a hierarchical modeling approach. The most important result is the ability to examine hypotheses related to size spectra, including the assessment of fixed and random effects, within a single Bayesian generalized (non)-linear mixed model.

SCHOLARONE™
Manuscripts

Bayesian hierarchical modeling of size spectra

Jeff S. Wesner[1], *Justin P.F. Pomeranz*[2], *James R. Junker*[3,4], *Vojsava Gjoni*[1], *Yuhlong Lio*[5]

[1]University of South Dakota, Department of Biology, Vermillion, SD 57069

[2]Colorado Mesa University, Environmental Science and Technology, Grand Junction, CO 81501

[3]Great Lakes Research Center, Michigan Technological University, Houghton, MI 49931

[4]Louisiana Universities Marine Consortium, Chauvin, LA 70344

[5]University of South Dakota, Department of Mathematics, Vermillion, SD 57069

Jeff.Wesner@usd.edu

Open Research Statement

All data, R code, and Stan code are available at https://github.com/jswesner/stan_isd (to be permanently archived at Zenodo upon acceptance).Body size data from the International Benthic Trawl Surveys was retrieved from https://github.com/andrew-edwards/sizeSpectra/tree/master/data.

For Review Only

Abstract

A fundamental pattern in ecology is that smaller organisms are more abundant than larger organisms. This pattern is known as the individual size distribution (ISD), which is the frequency of all individual sizes in an ecosystem, regardless of taxon. The ISD is described by power law distribution with the form $f(x) = Cx^{\lambda}$, and a major goal of size spectra analyses is to estimate the ISD parameter λ. However, while numerous methods have been developed to do this, they have focused almost exclusively on estimating λ from single samples. Here, we develop an extension of the truncated Pareto distribution within the probabilistic modeling language Stan. We use it to estimate multiple ISD parameters simultaneously with a hierarchical modeling approach. The most important result is the ability to examine hypotheses related to size spectra, including the assessment of fixed and random effects, within a single Bayesian generalized (non)-linear mixed model.

Keywords: *Bayesian, body size spectra, hierarchical, Pareto, power law, Stan*

For Review Only

Introduction

In any ecosystem, large individuals are typically more rare than small individuals. This fundamental feature of ecosystems leads to a remarkably common pattern in which relative abundance declines with individual body size, generating the individual size distribution (ISD), also called the community size spectrum (Sprules et al. 1983, White et al. 2008). Understanding how body sizes are distributed has been a focus in ecology for over a century (Peters and Wassenberg 1983), in part because they represent an ataxic approach that reflects fundamental measures of ecosystem structure and function, such as trophic transfer efficiency. (Kerr and Dickie 2001, White et al. 2007, Perkins et al. 2019). Individual size distributions are also predicted as a result of physiological limits associated with body size, thereby emerging from predictions of metabolic theory and energetic equivalence (Brown et al. 2004).

More formally, the ISD is a frequency distribution that can be approximated by a bounded power law with a single free parameter λ, corresponding to the following probability density function (Edwards et al. 2020):

$$f(x) = Cx^{\lambda}, x_{min} \leq x \geq x_{max} \tag{1}$$

where x is the body size (e.g., mass or volume) of an individual regardless of taxon, x_{min} is the smallest individual attainable and x_{max} is the largest possible individual (White et al. 2008). C is a constant equal to:

$$C = \begin{cases} \frac{\lambda+1}{x_{max}^{\lambda+1} - x_{min}^{\lambda+1}}, \lambda \neq -1 \\ \frac{1}{logx_{max} - logx_{min}}, \lambda = -1 \end{cases} \tag{2}$$

This model is also known as the bounded power law or truncated Pareto distribution. The terms "bounded" or "truncated" refer to the limits of x_{min} and x_{max}, which represent the minimum and maximum attainable body size values (White et al. 2008). In practice, values of x_{min} and x_{max}

For Review Only

often come from the minimum and maximum body sizes in a data set or are estimated statistically (White et al. 2008, Edwards et al. 2017).

A compelling feature of size spectra is that λ may vary little across ecosystems as a result of physiological constraints that lead to size-abundance patterns more broadly. Metabolic scaling theory predicts $\lambda + 1 = \frac{log10\alpha}{log10\beta} - 3/4$, where α is trophic transfer efficiency in the food web and β is the mean predator-prey mass ratio (Reuman et al. 2008). The value of $-3/4$ is the predicted scaling exponent of log abundance and log mass (Damuth 1981, Peters and Wassenberg 1983). It is the reciprocal of scaling coefficient of metabolic rate and mass (0.75) (Brown et al. 2004) and as a result, values of $\lambda + 1$ have been used to estimate metabolic scaling across ecosystems (Reuman et al. 2008, Perkins et al. 2018, 2019). Because $\frac{log10\alpha}{log10\beta}$ is typically «0.01, this implies that a λ values of ~-1.75 represent a reasonable first guess of expected ISD exponents, with values of ranging from -1.2 to -2 often appearing in the literature (Andersen and Beyer 2006, Blanchard et al. 2009, Pomeranz et al. 2020b).

Whether λ represents a fixed or variable value is debated, but it often varies among samples and ecosystems (Blanchard et al. 2009, Perkins et al. 2018, Pomeranz et al. 2020b). It is often described by its "steepness", with more negative values (i.e., "steeper") indicating lower abundance of large relative to small individuals, and vice versa. These patterns of size frequency are an emergent property of demographic processes (e.g., age-dependent mortality), ecological interactions (e.g., size-structured predation, trophic transfer efficiency), and physiological constraints (e.g., size-dependent metabolic rates) (Muller-Landau et al. 2006, Andersen and Beyer 2006, White et al. 2008). As a result, variation in λ across ecosystems or across time can indicate fundamental shifts in community structure or ecosystem functioning. For example, overfishing in marine communities has been detected using size spectra in which λ was steeper than expected, indicating fewer large fish than expected (Jennings and Blanchard 2004). Shifts in λ have also been used to document responses to acid mine drainage in streams (Pomeranz et al. 2019, 2020a), land use (Martínez et al. 2016), resource subsidies (Perkins et al. 2018), and temperature (O'Gorman et al. 2017, Pomeranz et al. 2022).

For Review Only

Given the ecological information it conveys, the data required to estimate size spectra are deceptively simple; only a single column of data are needed, in which each data point is a single measure of the body size of an individual. As long as the body sizes are collected systematically and without bias towards certain taxa or phenotypes, there is no need to know any more ecological information about the data points (e.g., taxon, trophic position, age, abundance). However, despite the simple data requirement, the statistical models used to estimate λ are diverse. Edwards et al. (2017) documented 8 different analytical methods. Six involved binning, in which the body sizes are grouped into size bins (e.g., 2-49 mg, 50-150 mg, etc.) and then counted, generating values for abundance within each size bin. When both axes are log-transformed, binning allows λ to be estimated using simple linear regression. Unfortunately, the binning process also removes most of the variation in the data, collapsing information about 1000's of individuals into just 6 or so bins. Doing so can lead to the wrong values of λ, sometimes drastically so (Goldstein et al. 2004, White et al. 2008, Pomeranz et al. 2023).

An improved alternative to binning and linear regression is to fit the body size data to a power law probability distribution (White et al. 2008, Edwards et al. 2017, 2020). This method uses all raw data observations directly to estimate λ, typically using the maximum likelihood estimation method (Edwards et al. 2017). In addition to estimating size spectra of single samples, ecologists have used this method to examine how λ varies across environmental gradients (Perkins et al. 2019, Pomeranz et al. 2022). However, these analyses typically proceed in two steps. First, λ estimates are obtained individually from each collection (e.g., each site or year, etc.). Second, these estimates are used as response variables in a linear model to examine how they relate to corresponding predictor variables (Edwards et al. 2020). A downside to this approach is that it treats body sizes (and subsequent λ's) as independent samples, even if they come from the same site or time. It also removes information on sample size (number of individuals) used to derive λ. As a result, the approach not only separates the data generation model from the predictor variables, but is also unable to take advantage of partial pooling during model fitting.

Here, we develop a Bayesian model that uses the truncated Pareto distribution to estimate λ in

For Review Only

response to both fixed and random predictor variables. The model extends the maximum likelihood approach developed by Edwards et al. (2020) and allows for a flexible hierarchical structure, including partial pooling, within the modeling language Stan (Stan Development Team 2022).

Methods

Translating to Stan

We first translated the probability density function described by Edwards et al. (2020) into Stan by converting it to the log probability density function (lpdf). Stan is a probabilistic modeling language that is capable of fitting complex models, including those with custom lpdf's. The resulting lpdf is given as

$$lpdf = \begin{cases} \log\frac{\lambda+1}{x_{max}^{\lambda+1}-x_{min}^{\lambda+1}} + \lambda \log x, \lambda \neq -1 \\ \text{-log}(\log x_{max} - \log x_{min}) - \log x, \lambda = -1 \end{cases} \quad (3)$$

with all variables as described above. We call this the $paretocustom$ distribution, which we can now use to estimate λ of a given data set. For example, an intercept-only model would look like this:

$$x_i \sim paretocustom(\lambda, x_{min}, x_{max})$$

$$\lambda = \alpha$$

$$\alpha \sim Normal(\mu, \sigma) \quad (4)$$

where x_i is the ith individual body size, λ is the size spectrum parameter (also referred to as the exponent), x_{min} and x_{max} are as defined above, and α is the intercept with a prior probability

For Review Only

distribution. In this case, we specified a Normal prior since λ is continuous and can be positive or negative, but this can be changed as needed.

The simple model above can be expanded to a generalized linear mixed model by including fixed predictors ($\beta\mathbf{X}$) and/or varying intercepts ($\alpha_{[x]}$):

$$
\begin{aligned}
x_{ij} &\sim paretocustom(\lambda_j, x_{min,j}, x_{max,j}) \\
\lambda &= \alpha + \beta\mathbf{X} + \alpha_{[j]} + \alpha_{[x]} \\
\alpha &\sim Normal(\mu_\alpha, \sigma_\alpha) \\
\beta &\sim Normal(\mu_\beta, \sigma_\beta) \\
\alpha_{[j]} &\sim Normal(0, \sigma_{[j]}) \\
\sigma_{[j]} &\sim Exponential(\phi) \\
\alpha_{[x]} &\sim Normal(0, \sigma_{[x]}) \\
\sigma_{[x]} &\sim Exponential(\phi)
\end{aligned} \tag{5}
$$

with one or more β regression parameters, represented by the vector β, for one or more fixed predictors $\mathbf{X}$, and one or more varying intercepts α_x. We specify α_j separately because it is needed to account for the non-independence of body sizes. In other words, each body size x_i is clustered within each site and so they are not independent and identically distributed. The addition of a varying intercept for each sample accounts for this non-independence. Prior distributions are given as $Normal$ for the parameters and varying intercept and $Exponential$ for $\sigma[x]$, but these can also be changed as needed.

The model above assumes that each body size x represents a single individual such that the data set might have many repeats for individuals of the same size (e.g., x = {0.2, 0.2, 0.2, 0.4, 0.4, 0.5, 9.8}). However, when individual body sizes are repeated in a data set, they are often accompanied

For Review Only

by a count or density, such that the data set above might instead consist of two columns with x = {0.2, 0.4, 0.5, 9.8} and $counts$ = {3, 2, 1, 1}. To analyze this more compact data set, Edwards et al. (2020) developed a modification of the log probability density function to include $counts$:

$$lpdf = \begin{cases} counts(\log\frac{\lambda+1}{x_{max}^{\lambda+1}-x_{min}^{\lambda+1}} + \lambda\log x), \lambda \neq -1 \\ counts(\text{-log}(\log x_{max} - \log x_{min}) - \log x, \lambda = -1 \end{cases} . \quad (6)$$

We refer to this as $paretocounts$, such that the model can be fit by using

$$x_i \sim paretocounts(\lambda, x_{min}, x_{max}, counts)$$

$$\lambda = [\text{linear or non-linear model}] \text{ and}$$

$$[\text{priors}]. \quad (7)$$

Aside from adding $counts$, the model is the same as presented above. These models ($paretocustom$ and $paretocounts$) allow us to test how the size distribution parameter, λ, varies in response to continuous or categorical predictors and to include hierarchical structure as needed.

Testing the models

The $paretocustom$ and $paretocounts$ lpdfs give the same results, differing only in how the data are aggregated. For simplicity, we demonstrate model performance here for the $paretocounts$ distribution, since the empirical data we used (see *Case Study* below) contains counts of individual body sizes. First, we tested for parameter recovery using data simulated from a bounded power law with known values of λ. Second, we fit the model to fisheries trawl data presented in Edwards et al. (2020) to estimate the hypothesis that λ declines over time.

For Review Only

Parameter recovery from simulated data

To ensure that the models could recover known parameter values, we simulated ten data sets from a bounded power law using the inverse cumulative density function:

$$x_i = (\mathrm{u}_i x_{max}^{(\lambda+1)} + (1 - \mathrm{u}_i) x_{min}^{(\lambda+1)})^{\frac{1}{(\lambda+1)}} \quad (8)$$

where x_i is the individual body size from the ith simulation, u_i is a unique draw from a $Uniform(0, 1)$ distribution, and all other variables are the same as defined above. We set x_{min} = 1, x_{max} = 1000, and simulated i = 1000 values from each of 10 λ's ranging from -2.2 to -1.2. To generate $counts$, we rounded each simulated value to the nearest 0.001 and then tallied them.

We estimated the ten λ values in two ways. First, we fit a separate intercept-only model to each of the ten data sets. Second, we fit a varying intercept model (Gelman et al. 2014). The structure of this model is $\lambda = \alpha + \alpha_{[group]}$ where each group represents an offset from the mean value of lambda.

Finally, we simulated data for a regression model with a single continuous predictor and a varying intercept: $\lambda = \alpha + \beta x + \alpha_{[group]}$, where α = -1.5, β = -0.1, and σ_{group} = 0.3. The predictor variable x was a continuous predictor. Using these parameters, we simulated 18 λ's, with each λ coming from one of three x-values (-2, 0, 2), nested within 3 groups with each replicated twice. From each λ, we simulated 1000 individuals using the procedure above, with x_{min} = 1 and x_{max} = 1000. Using those 18,000 simulated body sizes (1000 sizes simulated from 18 λ's), we fit a $paretocounts$ regression model 40 times to measure variation in parameter recovery among model runs.

Sample Size

We examined sensitivity to sample size (number of individual body sizes) across three λ values (-2, -1.6, -1.2). For each λ, we varied the number of simulated individuals from 2 to 2048, representing

For Review Only

a 2^n sequence with n ranging from 1 to 11. Each of the 11 densities was replicated 10 times resulting in 110 datasets of individual body sizes. We fit each data set using separate intercept-only $paretocounts$ models and then plotted the resulting λ values as a function of sample size.

Case Studies

To examine model performance on empirical data, we re-ran a previously published analysis from Edwards et al. (2020). In Edwards' study, size spectra parameters were first estimated separately for each sample using maximum likelihood. Then the modeled parameters were used as response variables in linear regression models. The goal was to test for linear changes in size spectra over three decades using bi-yearly size data of marine fishes collected from the International Benthic Trawl Survey (IBTS). The data set and original model results are available in the `sizeSpectra` package (Edwards et al. 2017). We tested the same hypothesis as Edwards et al. (2020), but instead of using a two-step process we fit a single model using the $paretocounts$ lpdf.

Model Fitting

We fit each of the above models in `rstan` (Stan Development Team 2022) using 2 chains each with 1000 iterations. All models converged with R_{hat}'s <1.01. If a known parameter value fell inside the 95% Credible Intervals, we considered parameter recovery successful. For the replicated regression model, we also tallied the number of times that the known value fell outside of the 95% CrI. Assessments of prior influence and model checking are available in Appendix S1.

Data Availability Statement

All data, R code, and Stan code are available at https://github.com/jswesner/stan_isd (to be permanently archived on acceptance).

For Review Only

Results

Parameter Recovery

For models fit to simulated individual data sets, all 95% credible intervals included the true value of λ and posterior medians were no more than 0.05 units away from the true value (Table 1). Similarly, when the same data set was fit using a varying intercepts model, the posterior median intercept α and group standard deviation σ_{group} were nearly identical to the true values (Table 1). Using the varying intercept model to estimate group specific means yielded similar results as using separate models per group (Figure 1a), demonstrating that a single model can be used to estimate multiple size spectra. The change from "shallow" to "steep" size spectra is also evident in plots of the proportion of values $\geq x$ (i.e., $f(x)$ from Eq. 1) (Figure 1b-d).

We also recovered regression parameters (α, β) along with the group-level standard deviation (σ_{group} (Figure 2). Thirty-seven of the 40 models converged. Of those 37 models the true value fell outside of the 95% CrI once for α and σ_{group} and three times for β (Figure 2). Averaging the deviations (posterior median minus the true value) among the replicates indicated no bias in the modeled estimates (mean bias $\pm$ sd: α = -0.01 $\pm$ 0.05, β = 0001 $\pm$ 0.004, σ_{group} = 0.02 $\pm$ 0.05).

Sample Size

Variation in modeled estimates was high for samples containing less than 100 individual (Figure 3). For example, when the true λ value was -2, samples with just 8 individuals yielded estimates ranging from -2.7 to -1.7. By contrast, all samples with more than 300 individuals captured the true λ with less than 0.1 unit of error (Figure 3).

For Review Only

Case Study

Using IBTS data (Edwards et al. 2017) with a Bayesian hierarchical regression, we found a negative trend over time. The ISD parameter of IBTS trawl data declined by ~0.001 units per year, but with a 95% CrI ranging from -0.005 to 0.002. These values were nearly identical to those reported by Edwards et al. (2020) using a two-step approach (Table 2). An advantage of fitting the model in a single Bayesian hierarchical framework is that estimates for individual groups are pulled toward the mean via partial pooling. This is apparent in comparing the unpooled MLE estimates (Figure 4a) to the partially pooled Bayesian estimates in each year (Figure 4b).

Discussion

The most important result of this work is the ability to analyze ISD parameters using fixed and random predictors in a hierarchical model. Our approach allows ecologists to test hypotheses about size spectra while avoiding the pitfalls of binning, which loses information and can lead to biased estimates of λ (White et al. 2008). Maximum likelihood solves this problem by directly estimating the ISD, but testing hypotheses with maximum likelihood is often done with a two-step process in which λ is estimated individually for each sample and the results are then used as response variables in linear or non-linear models (Edwards et al. 2020). Our approach merges these steps, allowing for the incorporation of prior probabilities and hierarchical structure.

The ability to incorporate prior information using Bayesian updating has two practical advantages over the two-step process described above. First, adding informative prior distributions can improve model fit by limiting the MCMC sampler to reasonable sampling space. In other words it would not be sensible to estimate the probability that λ is -1,234 or -9. Without informative priors, those values (and more extreme values) are considered equally likely and hence waste much of the algorithm's sampling effort on unlikely values (e.g., (Wesner and Pomeranz 2021)).

Second, and most importantly, ecologists have much prior information on the values that λ can take.

For Review Only

For example, global analysis of phytoplankton reveals values of -1.75, consistent with prediction based on sub-linear scaling of metabolic rate with mass of -3/4 (Perkins et al. 2019). Alternatively, Sheldon's conjecture suggests that λ is -2.05 (Andersen et al. 2006), a value reflecting isometric scaling of metabolic rate and mass, with support in pelagic marine food webs (Andersen and Beyer 2006). However, benthic marine systems typically have shallower exponents (e.g., $\sim$ -1.4; Blanchard et al. (2009)), similar to those in some freshwater stream ecosystems (-(Pomeranz et al. 2022). While the causes of these deviations from theoretical predictions are debated, it is clear that values of λ are restricted to a relatively narrow range between about -2.05 and -1.2. But this restriction is not known to the truncated Pareto, which has no natural lower or upper bounds on λ (White et al. 2008). As a result, a prior that places most of its probability mass on these values (e.g., $Normal(-1.75, 0.2)$ seems appropriate. Such a continuous prior does not prevent findings of larger or smaller λ, but instead places properly weighted skepticism on such values.

Similar to priors, partial pooling from varying intercepts provides additional benefits, allowing for the incorporation of hierarchical structure and pulling λ estimates towards the global mean (Gelman 2005, Qian et al. 2010). In the examples shown here, the amount of pooling is relatively small because the sample sizes are large (>1000 individuals). However, the primary benefit of pooling (both from varying effects and skeptical priors) is in prediction (Gelman 2005, Hobbs and Hooten 2015). This becomes especially important when models are used to forecast future ecosystem conditions. Forecasts are becoming more common in ecology (Dietze et al. 2018) and are likely to be easier to test with modern long-term data sets like NEON (National Ecological Observatory Network) in which body size samples will be collected at the continental scale over at least the next 20 years (Kuhlman et al. 2016). In addition, because the effects of priors and pooling increase with smaller samples sizes, varying intercepts are likely to be particularly helpful for small samples. In other words, priors and partial pooling contain built-in skepticism of extreme values, ensuring the maxim that "extraordinary claims require extraordinary evidence".

One major drawback to the Bayesian modeling framework here is time. Bayesian models of even minimal complexity must be estimated with Markov Chain Monte Carlo techniques. In this study,

For Review Only

we used the No U-Turn sampling (NUTS) algorithm via `rstan` (Stan Development Team 2022). Stan can be substantially faster than other commonly used programs such as JAGS and WinBUGS, which rely on Gibbs sampling. For example, Stan is 10 to 1000 times more efficient than JAGS or WinBUGS, with the differences becoming greater as model complexity increases (Monnahan et al. 2017). In the current study, intercept-only models for individual samples with $\sim$ 300 to 1500 individuals could be fit quickly (<2 seconds total run time (warm-up + sampling on a Lenovo T490 with 16GB RAM)) with as little as 1000 iterations and two chains. However, the IBTS regression models took >2 hours to run with the same iterations and chains. These times include the fact that our models used several optimization techniques, such as informative priors, standardized predictors, and non-centered parameterization, each of which are known to improve convergence and reduce sampling time (McElreath 2016). But if Bayesian inference is desired, these run-times may be worth the wait. In addition, they are certain to become faster with the refinement of existing algorithms and the introduction of newer ones like Microcanonical HMC (Robnik et al. 2022).

Body size distributions in ecosystems have been studied for decades, yet comprehensive analytical approaches to testing these hypotheses are lacking. We present a single analytical approach that takes advantage of the underlying data structures of individual body sizes (Pareto distributions) while placing them in a generalized (Non)-linear hierarchical modeling framework. We hope that ecologists will adopt and improve on the models here to critically examine hypotheses of size spectra or other power-law distributed data.

Acknowledgements

This material is based upon work supported by the National Science Foundation under Grant Nos. 2106067 to JSW and 2106068 to JRJ. We especially thank Edwards et al. (2017) and (2020) for placing their code and data in easily accessible repositories.

For Review Only

References

Andersen, K. H., and J. E. Beyer. 2006. Asymptotic Size Determines Species Abundance in the Marine Size Spectrum. The American Naturalist 168:54–61.

Blanchard, J. L., S. Jennings, R. Law, M. D. Castle, P. McCloghrie, M.-J. Rochet, and E. Benoît. 2009. How does abundance scale with body size in coupled size-structured food webs? Journal of Animal Ecology 78:270–280.

Brown, J. H., J. F. Gillooly, A. P. Allen, V. M. Savage, and G. B. West. 2004. Toward a metabolic theory of ecology. Ecology 85:17711789.

Damuth, J. 1981. Population density and body size in mammals. Nature 290:699–700.

Dietze, M. C., A. Fox, L. M. Beck-Johnson, J. L. Betancourt, M. B. Hooten, C. S. Jarnevich, T. H. Keitt, M. A. Kenney, C. M. Laney, L. G. Larsen, and others. 2018. Iterative near-term ecological forecasting: Needs, opportunities, and challenges. Proceedings of the National Academy of Sciences 115:1424–1432.

Edwards, A. M., J. P. W. Robinson, J. L. Blanchard, J. K. Baum, and M. J. Plank. 2020. Accounting for the bin structure of data removes bias when fitting size spectra. Marine Ecology Progress Series 636:19–33.

Edwards, A. M., J. P. W. Robinson, M. J. Plank, J. K. Baum, and J. L. Blanchard. 2017. Testing and recommending methods for fitting size spectra to data. Methods in Ecology and Evolution 8:57–67.

Gelman, A. 2005. Analysis of variance—why it is more important than ever. The Annals of Statistics 33:1–53.

Goldstein, M. L., S. A. Morris, and G. G. Yen. 2004. Problems with fitting to the power-law distribution. The European Physical Journal B-Condensed Matter and Complex Systems 41:255–258.

Hobbs, N. T., and M. B. Hooten. 2015. Bayesian models: A statistical primer for ecologists. Princeton University Press.

Jennings, S., and J. L. Blanchard. 2004. Fish abundance with no fishing: Predictions based on

For Review Only

macroecological theory. Journal of Animal Ecology:632–642.

Kerr, S. R., and L. M. Dickie. 2001. The biomass spectrum: A predator-prey theory of aquatic production. Columbia University Press.

Kuhlman, M. R., H. W. Loescher, R. Leonard, R. Farnsworth, T. E. Dawson, and E. F. Kelly. 2016. A New Engagement Model to Complete and Operate the National Ecological Observatory Network. The Bulletin of the Ecological Society of America 97:283–287.

Martínez, A., A. Larrañaga, A. Miguélez, G. Yvon-Durocher, and J. Pozo. 2016. Land use change affects macroinvertebrate community size spectrum in streams: the case of *Pinus radiata* plantations. Freshwater Biology 61:69–79.

McElreath, R. 2016. Statistical rethinking: A bayesian course with examples in R and stan. Second. CRC Press.

Monnahan, C. C., J. T. Thorson, and T. A. Branch. 2017. Faster estimation of Bayesian models in ecology using Hamiltonian Monte Carlo. Methods in Ecology and Evolution 8:339–348.

Muller-Landau, H. C., R. S. Condit, K. E. Harms, C. O. Marks, S. C. Thomas, S. Bunyavejchewin, G. Chuyong, L. Co, S. Davies, R. Foster, and others. 2006. Comparing tropical forest tree size distributions with the predictions of metabolic ecology and equilibrium models. Ecology letters 9:589–602.

O'Gorman, E. J., L. Zhao, D. E. Pichler, G. Adams, N. Friberg, B. C. Rall, A. Seeney, H. Zhang, D. C. Reuman, and G. Woodward. 2017. Unexpected changes in community size structure in a natural warming experiment. Nature Climate Change 7:659–663.

Perkins, D. M., I. Durance, F. K. Edwards, J. Grey, A. G. Hildrew, M. Jackson, J. I. Jones, R. B. Lauridsen, K. Layer-Dobra, M. S. A. Thompson, and G. Woodward. 2018. Bending the rules: Exploitation of allochthonous resources by a top-predator modifies size-abundance scaling in stream food webs. Ecology Letters 21:1771–1780.

Perkins, D. M., A. Perna, R. Adrian, P. Cermeño, U. Gaedke, M. Huete-Ortega, E. P. White, and G. Yvon-Durocher. 2019. Energetic equivalence underpins the size structure of tree and phytoplankton communities. Nature Communications 10:255.

For Review Only

Peters, R. H., and K. Wassenberg. 1983. The effect of body size on animal abundance. Oecologia 60:89–96.

Pomeranz, J. P. F., J. R. Junker, and J. S. Wesner. 2022. Individual size distributions across North American streams vary with local temperature. Global Change Biology 28:848–858.

Pomeranz, J. P. F., H. J. Warburton, and J. S. Harding. 2019. Anthropogenic mining alters macroinvertebrate size spectra in streams. Freshwater Biology 64:81–92.

Pomeranz, J. P. F., J. S. Wesner, and J. S. Harding. 2020a. Changes in stream food-web structure across a gradient of acid mine drainage increase local community stability. Ecology 101:e03102.

Pomeranz, J. P., J. R. Junker, V. Gjoni, and J. S. Wesner. 2023. Detecting differences in size spectra. bioRxiv:2023–03.

Pomeranz, J., J. S. Wesner, and J. S. Harding. 2020b. Changes in stream food-web structure across a gradient of acid mine drainage increases local community stability. Ecology.

Qian, S. S., T. F. Cuffney, I. Alameddine, G. McMahon, and K. H. Reckhow. 2010. On the application of multilevel modeling in environmental and ecological studies. Ecology 91:355–361.

Reuman, D. C., C. Mulder, D. Raffaelli, and J. E. Cohen. 2008. Three allometric relations of population density to body mass: Theoretical integration and empirical tests in 149 food webs. Ecology Letters 11:1216–1228.

Robnik, J., G. B. De Luca, E. Silverstein, and U. Seljak. 2022, December. Microcanonical Hamiltonian Monte Carlo. arXiv.

Sprules, W. G., J. M. Casselman, and B. J. Shuter. 1983. Size Distribution of Pelagic Particles in Lakes. Canadian Journal of Fisheries and Aquatic Sciences 40:1761–1769.

Stan Development Team. 2022. RStan: The R interface to Stan.

Wesner, J. S., and J. P. F. Pomeranz. 2021. Choosing priors in Bayesian ecological models by simulating from the prior predictive distribution. Ecosphere 12.

White, E. P., B. J. Enquist, and J. L. Green. 2008. On Estimating the Exponent of Power-Law Frequency Distributions. Ecology 89:905–912.

For Review Only

362 White, E. P., S. K. M. Ernest, A. J. Kerkhoff, and B. J. Enquist. 2007. Relationships between body
363 size and abundance in ecology. Trends in Ecology & Evolution 22:323–330.

For Review Only

Tables

Table 1: Table 1. Parameter recovery of the same data using two approaches. First, ten separate models individually recapture known lambda values. Second, the same ten data sets are estimated in a single hierarchical model. The true values are compared to the posterior median and 95% Credible Intervals.

Model	Parameter	True Value	q2.5	q50	q97.5
Separate Models	λ	-2.20	-2.23	-2.15	-2.08
Separate Models	λ	-2.09	-2.15	-2.09	-2.02
Separate Models	λ	-1.98	-2.08	-2.02	-1.96
Separate Models	λ	-1.87	-1.93	-1.87	-1.81
Separate Models	λ	-1.76	-1.75	-1.70	-1.65
Separate Models	λ	-1.64	-1.65	-1.60	-1.56
Separate Models	λ	-1.53	-1.54	-1.50	-1.46
Separate Models	λ	-1.42	-1.45	-1.42	-1.38
Separate Models	λ	-1.31	-1.34	-1.30	-1.26
Separate Models	λ	-1.20	-1.23	-1.20	-1.16
Single Model with Varying Intercepts	α	-1.70	-1.96	-1.71	-1.50
Single Model with Varying Intercepts	σ_[group]	0.34	0.23	0.36	0.58

For Review Only

Table 2: Table 2. Slope values from a regression testing the relationship between the ISD exponent and year for IBTS trawl data (Edwards et al. 2020). The values are derived using the Bayesian hierarchical model presented here or from the maximum likelihood approach described in Edwards et al. (2020).

Model	Mean	q2.5	q97.5
Bayesian - one step	-0.001	-0.005	0.002
MLE - two steps	-0.001	-0.005	0.003

For Review Only

Figure Captions

Figure 1. a) Modeled estimates (median +/- 95% Credible Intervals) of λ using either 10 separate models or a single model with ten varying intercepts. c-d) Fit of ISD relationships at 3 values of λ. Dots are raw data, lines are posterior medians, and shading is the 95% credible interval. Fits are from separate models.

Figure 2. Posterior distributions of n = 40 modeled estimates of alpha, beta, and sigma_group for a linear regression estimating the size spectrum exponent as a function of a continuous predictor. All data were simulated. Gray densities indicate that the 95% CrI contains the true value, while black densities indicate the true values fall outside of the CrI. The vertical lines indicate true values.

Figure 3. Estimates of λB across 11 different sample sizes (ranging from 2 to 2048 individuals) and three different true λ's (-2, -1.6, -1.2). Ten separate models were fit for each of the 11 sample sizes. The horizontal lines show the true value of λ.

Figure 4. Regression results from a) Edwards et al. (2020) using maximum likelihood and linear regression (two steps) and b) the Bayesian model with varying intercepts. In a) the points represent maximum likelihood estimates calculated separately for each year. In b) they represent hierarchical varying intercepts calculated from the model.

For Review Only

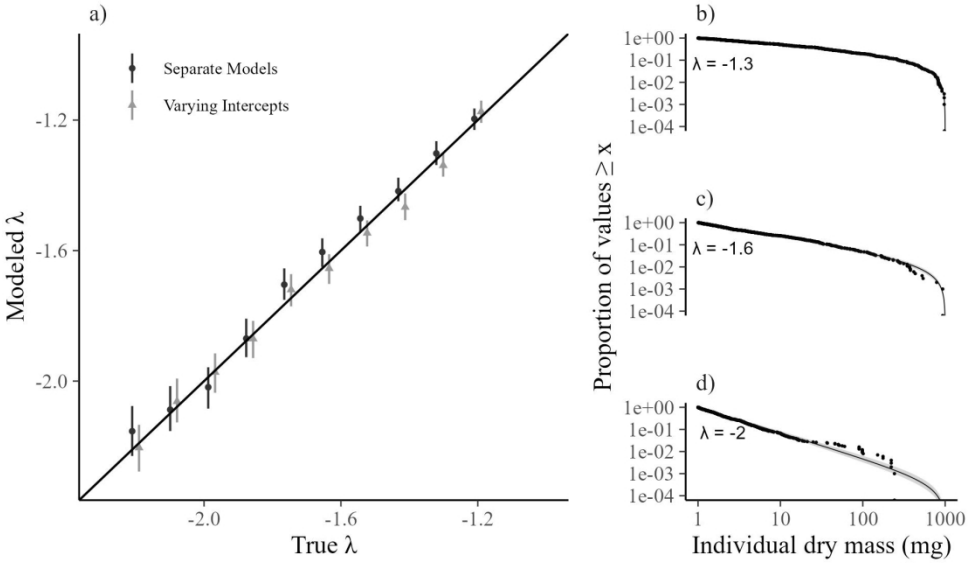

Figure 1

687x423mm (72 x 72 DPI)

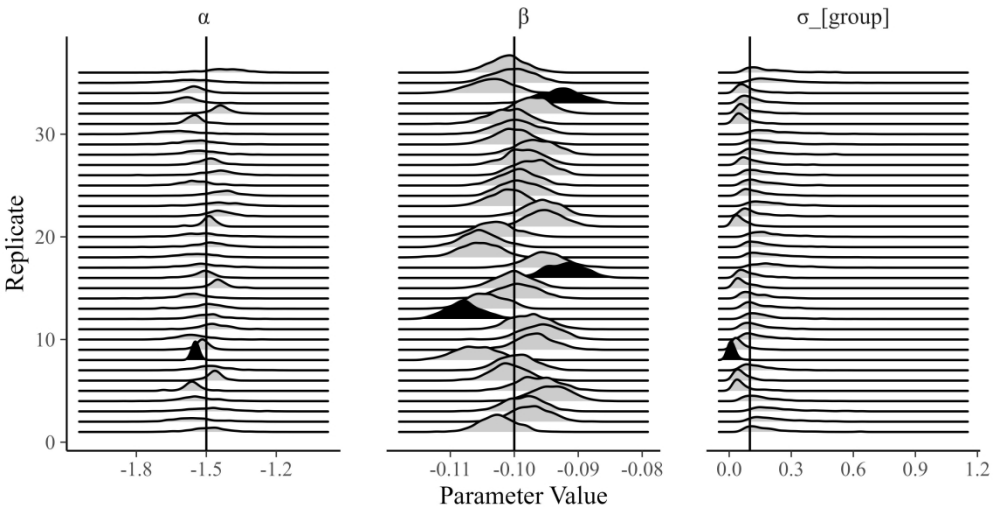

Figure 2

1375x740mm (72 x 72 DPI)

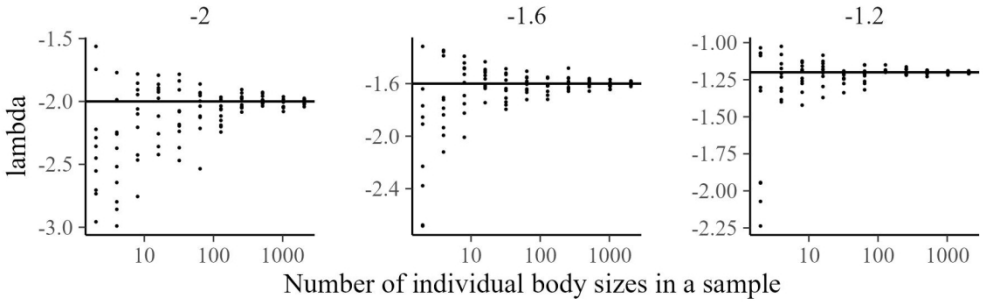

Figure 3

635x211mm (72 x 72 DPI)

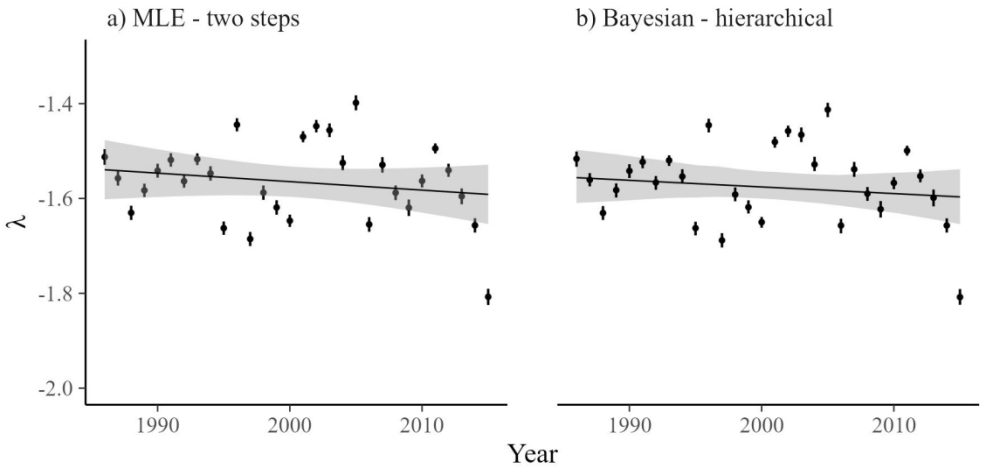

Figure 4

635x317mm (72 x 72 DPI)

Supplementary Information: Bayesian hierarchical modeling of size spectra

Jeff S. Wesner[1], Justin P.F. Pomeranz[2], James R. Junker[3,4], Vojsava Gjoni[1], and Yuhlong Lio[5]

Journal: *Ecology*

[1] University of South Dakota, Department of Biology, Vermillion, SD 57069

[2] Colorado Mesa University, Environmental Science and Technology, Grand Junction, CO 81501

[3] Great Lakes Research Center, Michigan Technological University, Houghton, MI 49931

[4] Louisiana Universities Marine Consortium, Chauvin, LA 70344

[5] University of South Dakota, Department of Mathematics, Vermillion, SD 57069

Correspondence: Jeff S. Wesner <Jeff.Wesner@usd.edu>

Appendix S1

Model Assessment

Model assessment is a key part of the Bayesian workflow, one goal of which is to assess prior influence and model fit (Conn et al. 2018, Gelman et al. 2020). Here, we provide examples of model assessment using the prior predictive distribution, a prior sensitivity analysis, and the posterior predictive distribution (Gabry et al. 2018). As model assessment is a broad and developing area (Conn et al. 2018), we do not intend this demonstration to be exhaustive, but merely to demonstrate it for the *paretocounts* lpdf models developed in the main manuscript.

Prior Predictive

Prior implications are often best understood through visualizations of the prior predictive distribution (Gabry et al. 2017; Wesner and Pomeranz 2021). We demonstrate that here by comparing prior and posterior distributions of a single ISD (Figure S1a,b). Figure S1a shows 30 ISD's simulated from a prior λ of *Normal*(-1.75, 0.2) (mean, sd). For this prior, most of the prior probability is centered between ~ -2.1 to -1.3, making it relatively weak prior that includes most

For Review Only

of the empirical ranges of ISD λ's. Using this prior, we fit the model to data simulated from a known λ = -1.5, with x_{min} = 1 and x_{max} = 1000. After fitting, the posterior is updated to *Normal*(-1.5, 0.02) (Figure S1b), recapturing the true λ with apparent minimal influence of the prior. Thirty draws from the prior or posterior are shown in Figure 1a,b.

Similarly, to understand the implications of a covariate prior in a regression model, we plotted 100 simulations of λ from the model:

$$x_{ij} \sim paretocounts(\lambda_j, x_{min,j}, x_{max,j}, counts)$$

$$\lambda = \alpha + \beta \text{year\_s} + \alpha_{[j]} + \alpha_{[x]}$$

$$\alpha \sim Normal(-1.5, 0.2)$$

$$\beta \sim Normal(0, 0.1)$$

$$\alpha_{[j]} \sim Normal(0, \sigma_{[j]})$$

$$\sigma_{[j]} \sim Exponential(2)$$

$$\alpha_{[x]} \sim Normal(0, \sigma_{[x]})$$

$$\sigma_{[x]} \sim Exponential(2)$$

where x_{ij} is the i^{th} individual from year j (with years standardized) and all other parameters as defined in the main text. The data for this model represent body sizes of fish captured over multiple years from the IBTS surveys as described in Edwards et al. (2017). The focus of this analysis is on the slope parameter β, which indicates the change in λ over time (years). Figure S1c shows the implied changes of λ from the prior for β of Normal (0, 0.1). This is a fairly informative prior as it keeps the predictions of λ within reasonable values (between ~-2 to -0.8) but is ambivalent on the direction of change (positive or negative). After fitting the model to data, the posterior is much more precise with the sd an order of magnitude smaller, indicating some support for a negative slope of -0.1.

For Review Only

Prior Sensitivity

The previous section demonstrated how to compare prior and posterior predictions. A separate question about priors is to understand how sensitive the resulting posteriors are to prior specifications. We can test sensitivity to prior choices by altering the prior for any or all parameters in the model and comparing the outcomes. Here, we created increasingly informative priors for λ by setting the Gaussian mean to -1.8 and reducing the standard deviation by orders of magnitude from 2 to 0.2, to 0.02. We then fit three ISD's to simulated data with a known λ of -1.98. With prior standard deviations of 2 and 0.2, the posterior λ's were similar, with credible intervals including the true value (Table S1). By contrast, when the prior is highly informative with a standard deviation of 0.01, it has a clear influence on the posterior, reducing it to a mean of -1.86 with 95% CrI that exclude both the true λ of the data and the prior λ.

Model Fit

Because Bayesian models are generative, we can assess model fit by simulating data from the posterior distribution and comparing it to the raw data (Gabry et al. 2018). The motivation for this approach is that a model that faithfully recaptures the data generation process should generate data that resemble the raw data in at least some aspects. We did this by first fitting ISD's to data generated from three known λ's (-2, -1.6, -1.3). Then we used the posterior predictive distribution to simulate 500 datasets and compare them to the raw data. We did this visually using boxplots (Figure S2a-c) of the raw data compared to the first 10 simulations of data from the posterior. In addition, we calculated the geometric mean (GM) of each simulation and the raw data using

$$GM_j^{(k)} = exp\left(\frac{1}{n}\sum_{i=1}^{n} \ln x_{ij}^{(k)}\right)$$

For Review Only

Where x_{ij} is the i^{th} body size from the j^{th} group, represented here by the different known lambdas used to simulate data (-2, -1.6 or -1.3). We generated a unique geometric mean for each of 500 posterior draws (k). We visualized discrepancies to the raw geometric mean using histograms compared to the raw geometric means (Figure S2d-f).

The results indicate good fit, showing that the posteriors generated from *paretocounts()* models strongly resemble the raw data (Figure S2a-c). In addition, the geometric means of the raw data were captured by the geometric means simulated from the posteriors (Figure S2d-f). One possible discrepancy appears in Figure S2f, where the true geometric mean is in the upper tail of the posterior histogram. A likely explanation for this is that the prior λ is set to $N(-1.8, 2)$, while the true λ in Figure S2f is -1.3. It is possible that the discrepancy is due to the prior influence, though this should be explored. The most important result of this is simply to demonstrate that standard model assessment applies to the power-law models presented here. For a more thorough treatment of model checking, see Gelman et al. (2014) and Conn et al. (2018).

For Review Only

Tables

Table S1: Prior sensitivity analysis showing how the posterior estimate of lambda changes as the prior standard deviation becomes more restrictive. The posteriors are summarized for models run on the same dataset containing 1000 simulated individuals from a true lambda of -1.98, xmin = 1, and xmax = 1000.

		Posterior			
True lambda	Prior(mean, sd)	Mean	SD	2.5%	97.5%
-1.98	N(-1.8, 2.00)	-2.02	0.03	-2.08	-1.96
-1.98	N(-1.8, 0.10)	-2.01	0.03	-2.07	-1.94
-1.98	N(-1.8, 0.01)	-1.86	0.02	-1.90	-1.83

For Review Only

84

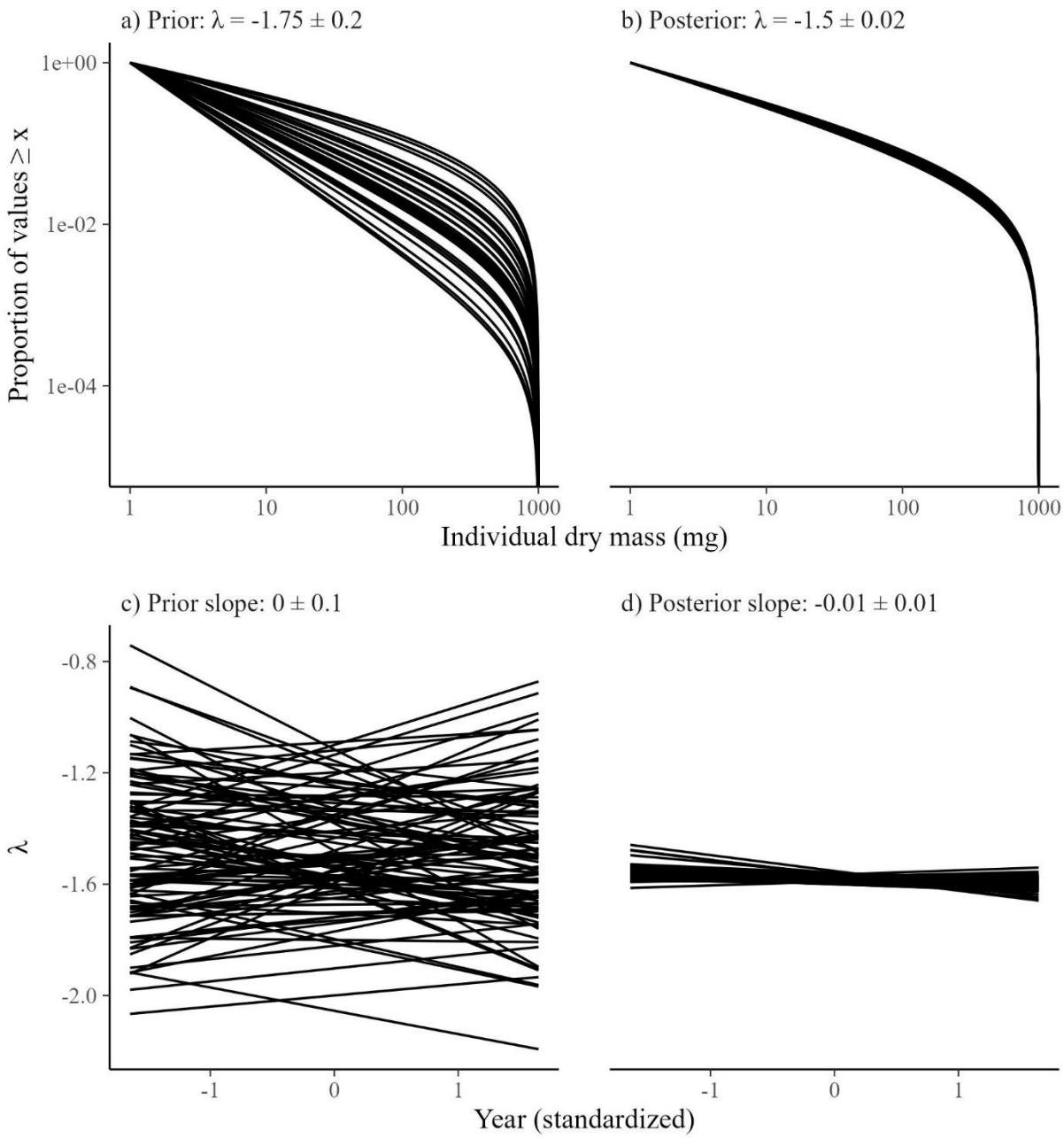

85
86 Figure S1. Thirty simulations from a) the prior distribution and b) the posterior distribution after
87 fitting the model to data. Each line represents a single draw from the prior or posterior
88 distributions (mean ±) sd).
89

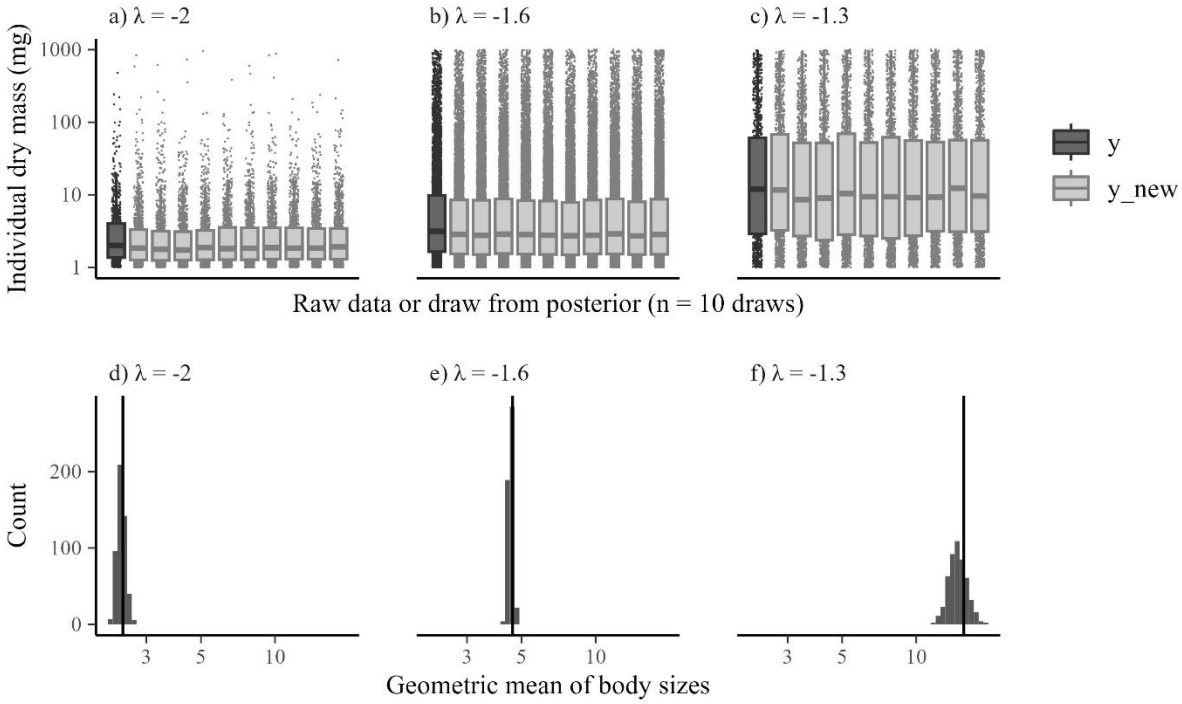

Figure S2. Posterior predictive checks of models estimating three ISD's with true λ's ranging from -2 to -1.3. a-c) Raw data and boxplots from the original data (y) and 10 simulated datasets from the posterior (y_new). d-f) Histograms of the geometric mean from 500 simulated datasets from the posterior compared to the geometric mean of the raw data (vertical line).

For Review Only

96

97 **References**

98 Conn, P. B., Johnson, D. S., Williams, P. J., Melin, S. R., & Hooten, M. B. (2018). A guide to
99 Bayesian model checking for ecologists. *Ecological Monographs*, *88*(4), 526-542.

100 Edwards, A. M., Robinson, J. P., Plank, M. J., Baum, J. K., & Blanchard, J. L. (2017). Testing
101 and recommending methods for fitting size spectra to data. *Methods in Ecology and*
102 *Evolution*, *8*(1), 57-67.

103 Gabry, J., Simpson, D., Vehtari, A., Betancourt, M., & Gelman, A. (2019). Visualization in
104 Bayesian workflow. *Journal of the Royal Statistical Society Series A: Statistics in*
105 *Society*, *182*(2), 389-402.

106 Gelman, A., Carlin, J. B., Stern, H. S., Dunson, D. B., Vehtari, A., & Rubin, D. B.
107 (2013). *Bayesian data analysis*. CRC press.

108 Gabry, J., Simpson, D., Vehtari, A., Betancourt, M., & Gelman, A. (2019). Visualization in
109 Bayesian workflow. *Journal of the Royal Statistical Society Series A: Statistics in*
110 *Society*, *182*(2), 389-402.

111 Wesner, J. S., & Pomeranz, J. P. (2021). Choosing priors in Bayesian ecological models by
112 simulating from the prior predictive distribution. *Ecosphere*, *12*(9), e03739.

For Review Only